J. Mechatron. Electr. Power Veh. Technol 07 (2016) 105-112

Journal of Mechatronics, Electrical Power, and Vehicular Technology

e-ISSN:2088-6985
p-ISSN: 2087-3379

www.mevjournal.com

ACCURACY ANALYSIS OF GEOMETRICAL AND NUMERICAL APPROACHES FOR TWO DEGREES OF FREEDOM ROBOT MANIPULATOR

Hendri Maja Saputra *, Midriem Mirdanies, Estiko Rijanto
Research Center for Electrical Power and Mechatronics, Indonesian Institute of Sciences,
Komplek LIPI, Jl. Sangkuriang, Gd. 20. Lt. 2, Bandung 40135, Indonesia

Received 28 October 2016; received in revised form 14 November 2016; accepted 15 November 2016
Published online 23 December 2016

Abstract

Analysis of algorithms to determine the accuracy of aiming direction using two inverse kinematic approaches *i.e.* geometric and numeric has been done. The best method needs to be specified to precisely and accurately control the aiming direction of a two degrees of freedom (TDOF) manipulator. The manipulator degrees of freedom are azimuth (Az) and elevation (El) angles. A program has been made using C language to implement the algorithm. Analysis of the two algorithms was done using statistical approach and circular error probable (CEP). The research proves that accuracy percentage of numerical method is better than geometrical method, those are 98.63% and 98.55%, respectively. Based on the experiment results, the numerical approach is the right algorithm to be applied in the TDOF robot manipulator.

Keywords: azimuth; elevation; geometrical; numerical; C language.

I. INTRODUCTION

Two degrees of freedom (TDOF) manipulator is a device that makes a modern instrument more convenient to be operated. Modern TDOF robot manipulator has been equipped with object detection and identifies features using certain sensors, such as acoustic sensors and visual sensors. In the study conducted by Mirdanies [1], object detection and identification was performed using Kinect™ camera with sift and surf methods.

Visual sensors and algorithm are used to convert the coordinates of the target to the aiming direction which is the key to this technology. The algorithm will determine the accuracy and precision of the TDOF manipulator aiming direction. The formula of this algorithm is closely associated with the forward and inverse kinematic as in the science of robotics [2]. Inverse kinematic can be completed with two common approaches, *i.e.* geometrical and numerical [3, 4] approaches. Robotic or mechatronic systems that use high-speed processing devices can use the numerical approach through an iterative process of Jacobian matrix for the inverse kinematic solution [5, 6]. Research on inverse kinematic via geometrical and numerical approach has been done by Feng [7] for PUMA 560, but the accuracy and precision issues are not discussed in detail. Especially for inverse kinematic via numerical approach, Tchon [8] has applied it to the stationary manipulators and mobile robots. In the numerical approach undertaken by Soch [9], the extended Jacobian technique has been compared with the inverse Jacobian. Kinect™ is used as a visual sensor in this study. It is placed on a fixed base so that coordinate transformation from a position of the manipulator is to be derived using the Denavit-Hartenberg (DH) notation [2].

This study aims to analyze the effect of using geometrical and numerical approaches to the accuracy and precision of a TDOF robot manipulator aiming direction.

II. HOMOGENEOUS TRANSFORMATION MATRIX

Figure 1 illustrates coordinates system of the camera, the TDOF manipulator, and the pointed

* Corresponding Author.Tel: +62 8138 1006 059
E-mail: hend018@lipi.go.id

 doi: 10.14203/j.mev.2016.v7.105-112.
Accreditation Number: (LIPI) 633/AU/P2MI-LIPI/03/2015 and (Ministry of RTHE) 1/E/KPT/2015.

direction of a specific target. Homogeneous transformation matrix of the camera can be written in the form of ZYX Euler representation ($^{A}_{B}R_{\alpha,\beta,\gamma}$) in combination with the translational vector [2]. Assuming that there is no change in orientation ($\alpha = \beta = \gamma = 0$) and there is only translation along the X-axis (Δ_x), Y-axis ($-\Delta_y$), and Z-axis (Δ_z) the homogeneous camera transformation T_c can be written as Equation (1).

$$T_C = \begin{bmatrix} 1 & 0 & 0 & \Delta_x \\ 0 & 1 & 0 & -\Delta_y \\ 0 & 0 & 1 & \Delta_z \\ 0 & 0 & 0 & 1 \end{bmatrix} \quad (1)$$

Based on direct measurements in the mechanism, it is known that Δ_x value is 26.5 cm, Δ_y is 1.25 cm, and Δ_z is 0 cm. The TDOF robot manipulator parameters in the DH notation [2] can be seen in Table 1. These parameters are used to calculate the coordinates of each point based on homogeneous transformations in Equation (2). The calculation results of each link are shown by Equation (3) and Equation (4). Homogeneous transformation matrix of the manipulator from the tip relative to the base coordinates can be seen in Equation (5).

$$^{i-1}_{i}T_m = \begin{bmatrix} c\,\theta_i & -s\,\theta_i\,c\,\alpha_i & s\,\theta_i\,s\,\alpha_i & a_i\,c\,\theta_i \\ s\,\theta_i & c\,\theta_i\,c\,\alpha_i & -c\,\theta_i\,s\,\alpha_i & a_i\,s\,\theta_i \\ 0 & s\,\alpha_i & c\,\alpha_i & d_i \\ 0 & 0 & 0 & 1 \end{bmatrix} (2)$$

$$^{0}_{1}T_m = \begin{bmatrix} c\,\theta_1 & 0 & s\,\theta_1 & 0 \\ s\,\theta_1 & 0 & -c\,\theta_1 & 0 \\ 0 & 1 & 0 & d_1 \\ 0 & 0 & 0 & 1 \end{bmatrix} \quad (2)$$

$$^{1}_{2}T_m = \begin{bmatrix} c\,\theta_2 & -s\,\theta_2 & 0 & a_2\,c\,\theta_2 \\ s\,\theta_2 & c\,\theta_2 & 0 & a_2\,s\,\theta_2 \\ 0 & 0 & 1 & 0 \\ 0 & 0 & 0 & 1 \end{bmatrix} \quad (3)$$

Table 1.
TDOF robot manipulator parameters

Link - i	αi	ai	di	θi
1	π/2	0	d_1	θ_1
2	0	a_2	0	θ_2

$$^{0}_{2}T_m = \begin{bmatrix} c\,\theta_1\,c\,\theta_2 & -c\,\theta_1\,s\,\theta_2 & s\,\theta_1 & a_2\,c\,\theta_1\,c\,\theta_2 \\ s\,\theta_1\,c\,\theta_2 & -s\,\theta_1\,s\,\theta_2 & -c\,\theta_1 & a_2\,s\,\theta_1\,c\,\theta_2 \\ s\,\theta_2 & c\,\theta_2 & 0 & d_1 + a_2\,s\,\theta_2 \\ 0 & 0 & 0 & 1 \end{bmatrix} (4)$$

where $s\,\theta_1 = \sin\theta_1$, $c\,\theta_1 = \cos\theta_1$, $s\,\theta_2 = \sin\theta_2$, and $c\,\theta_2 = \cos\theta_2$. d_1 represents length of link 1, and a_2 is length of link 2. Based on measurements, it is known that d_1 is 34.25 cm, whereas a_2 is 40 cm.

The targets are assumed to be simply a translation along the X-axis (L_x), thus homogeneous transformation matrix of the target referred to the tip of the link 2 can be written as Equation (6).

$$T_T = \begin{bmatrix} 1 & 0 & 0 & L_x \\ 0 & 1 & 0 & 0 \\ 0 & 0 & 1 & 0 \\ 0 & 0 & 0 & 1 \end{bmatrix} \quad (5)$$

The total homogeneous transformation matrix is obtained by multiplying homogeneous transformation matrix of the camera, the manipulator, and the target matrix as follows:

$$T = T_C * {}^{0}_{2}T_m * T_T = \begin{bmatrix} R & P \\ 0 & 1 \end{bmatrix} \quad (6)$$

where

$$R = \begin{bmatrix} n_x & s_x & a_x \\ n_y & s_y & a_y \\ n_z & s_z & a_z \end{bmatrix} = \begin{bmatrix} c\,\theta_1\,c\,\theta_2 & -c\,\theta_1\,s\,\theta_2 & s\,\theta_1 \\ s\,\theta_1\,c\,\theta_2 & -s\,\theta_1\,s\,\theta_2 & -c\,\theta_1 \\ s\,\theta_2 & c\,\theta_2 & 0 \end{bmatrix} \quad (7)$$

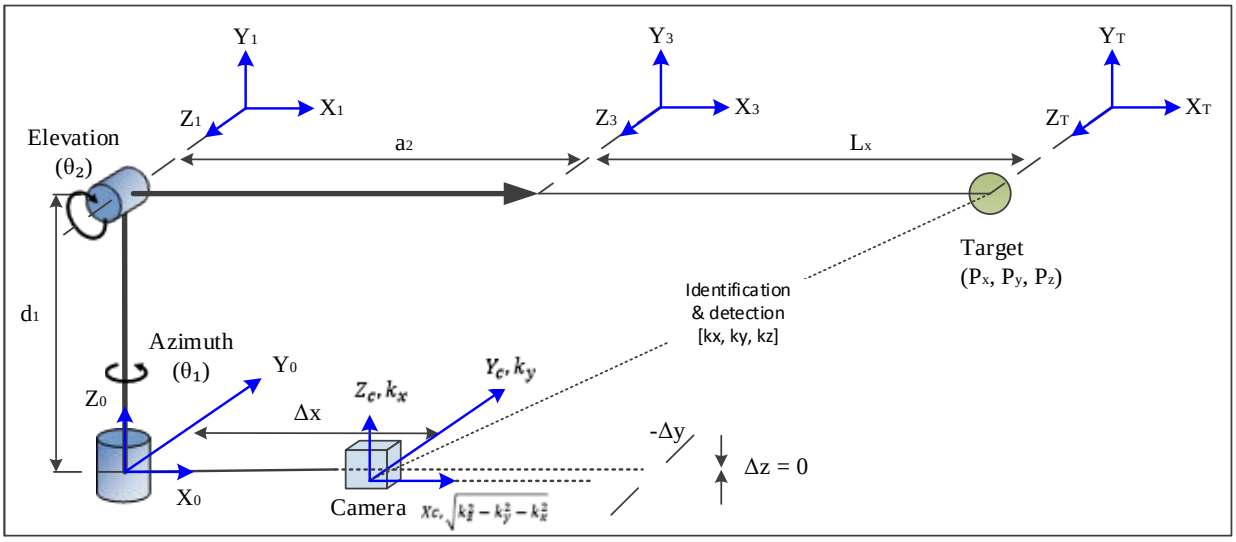

Figure 1. Coordinates system of camera, TDOF manipulator, and target point

$$P = \begin{bmatrix} (a_2 + L_x) & c\,\theta_1\, c\,\theta_2 \\ (a_2 + L_x) & s\,\theta_1\, c\,\theta_2 \\ d_1 + (a_2 + L_x) & s\,\theta_1 \end{bmatrix} + \begin{bmatrix} \Delta_x \\ -\Delta_y \\ \Delta_z \end{bmatrix} \quad (8)$$

III. INVERSE KINEMATICS

Coordinates system of the camera, as shown in Figure 1, the object being detected by the camera is expressed in the camera coordinate system as [k_x, k_y, k_z]. In the camera coordinate system, Z-axis forms a straight line between the camera and the object, and kz represents the distance between them in Z-axis. Therefore, the coordinates of the object in the DH-coordinate system is given by the following equation:

$$P_d = \begin{bmatrix} P_x \\ P_y \\ P_z \end{bmatrix} = \begin{bmatrix} \sqrt{k_z^2 - k_y^2 - k_x^2} + \Delta_x \\ k_x - \Delta_y \\ k_y + \Delta_z \end{bmatrix} \quad (9)$$

A. Geometrical Approach

Figure 2 illustrates coordinates system which is used to derive inverse kinematics using geometrical approach. From trigonometric formula, the following equations are obtained [3].

$$\left.\begin{aligned} \theta_1 &= \tan^{-1}\left(\frac{P_y}{P_x}\right) \\ \theta_2 &= \tan^{-1}\left(\frac{z}{r}\right) = \tan^{-1}\left(\frac{P_z - d_1}{\sqrt{P_x^2 + P_y^2}}\right) \end{aligned}\right\} \quad (10)$$

where θ_1 is a rotation of joint on the horizontal plane which is called azimuth angle, θ_2 is a rotation of joint on the vertical plane which is called elevation angle, (P_x, P_y, P_z) is the target coordinates relative to the manipulator base coordinate, and (d_1, a_2) is the length of the link 1 and link 2, respectively.

The distance L from the second joint to the target can be calculated as follows:

$$L = a_2 + L_x = \sqrt{P_x^2 + P_y^2 + (P_z - d_1)^2} \quad (11)$$

B. Numerical Approach

The algorithm of numerical approach is carried out through iteration process using pseudo-inverse Jacobian matrix [1] as Figure 3.

IV. ACCURACY MEASUREMENT

In general, imprecise measurement is associated with random errors while the inaccurate measurement is associated with systematic errors. Good aiming results will have small systematic and random errors, and vice versa. Systematic errors values are expressed by the difference between the average results of the aim with the midpoint of the target value, while the random errors value is determined by the value of the standard deviation from the results of the aim [10].

Data can be analyzed under the assumption Gaussian (normal) distribution and independent of each other [11]. Gaussian is a distribution of data whose characteristics matches a probability density function (PDF) with average (mean) μ and variance σ^2. Experiment results are data sets of points in the horizontal axis (x) and the vertical axis (y) in a window area generated by a laser pointer.

Once the impact point distribution has been assumed to be normal and independent in both dimensions, the dispersion of aiming points can be described using the circular error probable (CEP) [12, 13, 14, 15]. The CEP is often used to measure the level of accuracy in many

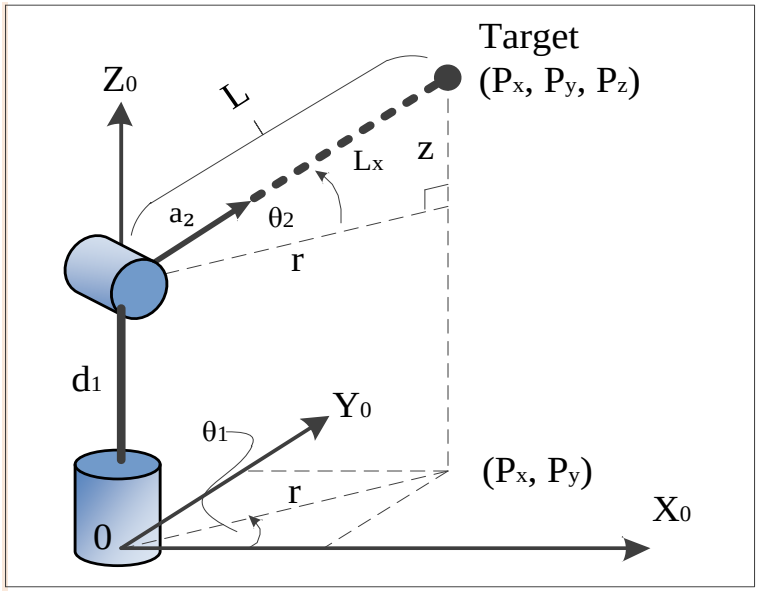

Figure 2. Geometrical approach coordinates

applications [12]. CEP is defined as the radius r of a circle, centered on the target, which includes 50% of the aiming points [13, 15]. Estimation of CEP is based on means and standard deviations

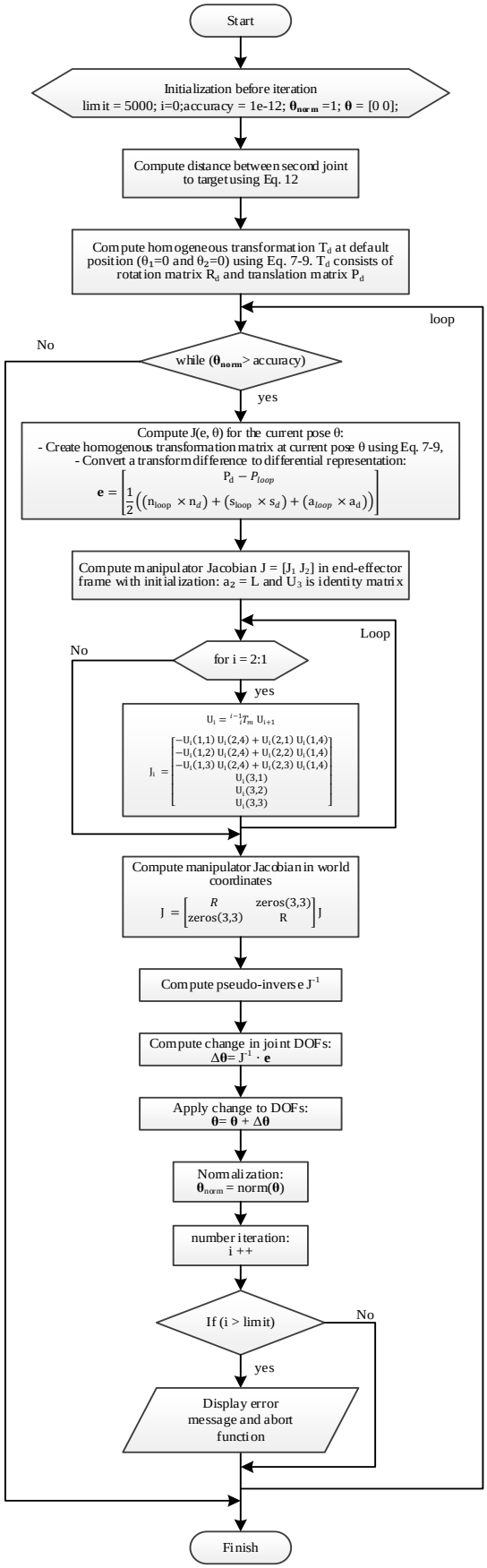

Figure 3. Numerical approach

[13]. The use of CEP must meet four criteria: independence, normality, circular distribution, and mean point of impact (MPI) at the target. These criteria can be determined based on the general statistical tests.

Independence and MPI use the Student-test, normality using the Lillifors test, and circular distribution using the F-Test. In the aim results that have sampled the standard deviation of the two coordinate axes, the CEP is calculated using Equation (13) [12].

$$CEP = \begin{cases} (0.820k - 0.007)\sigma_s + 0.675\sigma_l & k < 0.3 \\ 0.615\sigma_s + 0.564\sigma_l & k \geq 0.3 \\ 1.177\sigma & k = 1 \end{cases} \quad (12)$$

where k is σ_s/σ_l , σ_s is the smaller standard deviation, σ_l is the larger standard deviation, and σ is σ_x or σ_y.

In this paper, accuracy **e** is expressed in the form of a percentage of accuracy level according to Equation (14).

$$\text{e } \% = \left(1 - \frac{\beta}{A}\right) \times 100\% \quad (13)$$

where β is radius of systematic error ($\beta = \sqrt{\bar{x} + \bar{y}}$) and A is maximum radius of aiming area.

V. EXPERIMENTAL SET-UP

The experimental set up is illustrated in Figure 4 and its working principle is shown in Figure 5. The target trajectory is represented by a linear and sinusoidal line input to produce movement of azimuth and elevation angles. It is given by the following equations:

$$\left.\begin{aligned} X_i &= X_{i-1} + 20, \text{for } 20 \leq X_i \leq 640 \\ Y_i &= A_y \sin(2\pi f X_i + \phi_y) + b \end{aligned}\right\} \quad (14)$$

where X_i and X_{i-1} are horizontal pixels along X-axis, Y_i is vertical pixel along Y-axis, A_y is sinusoidal gain, f is frequency, and b is offset.

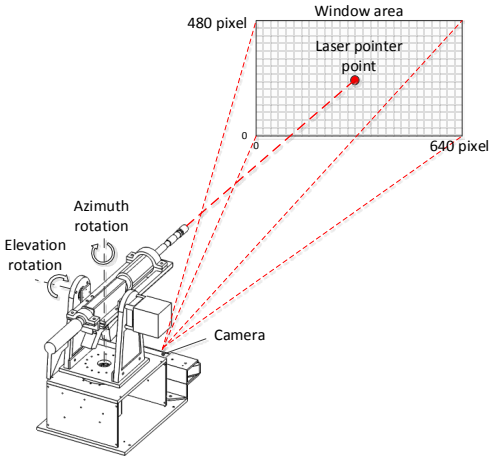

Figure 4. Experimental set-up. The heading direction is represented by a laser pointer on the window area (640x480 pixel) to be captured by the camera

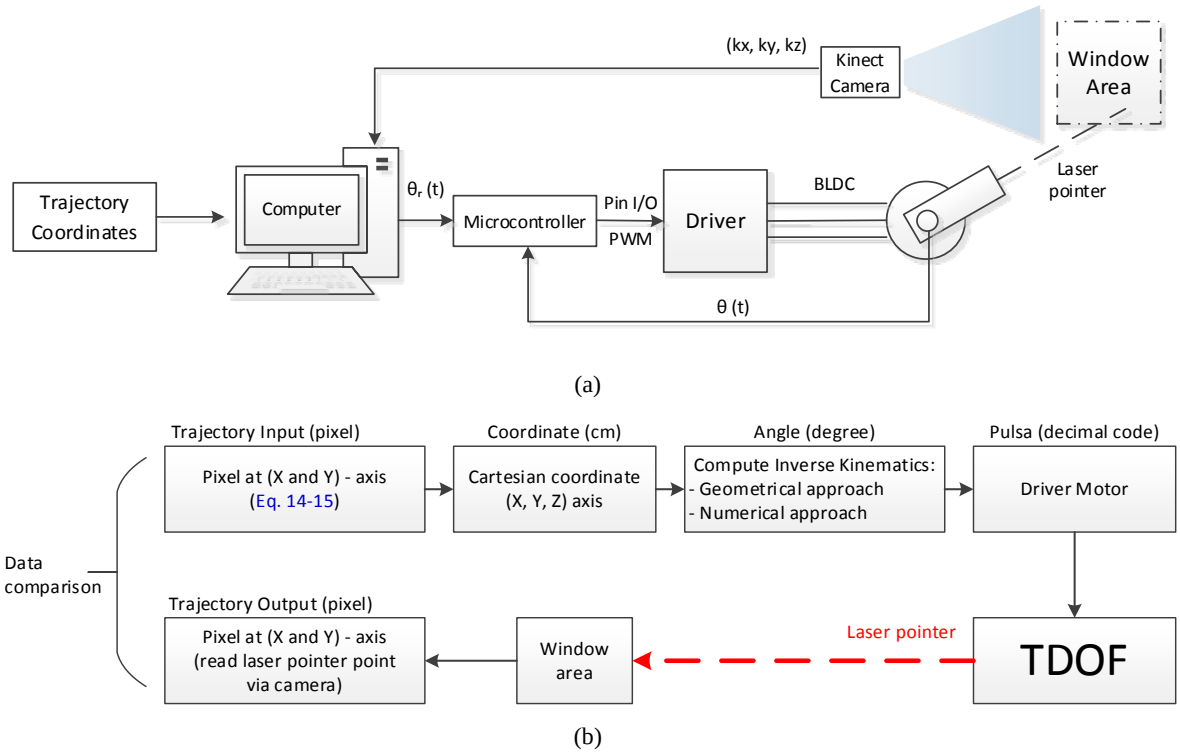

Figure 5. The working principle of experiment: (a) Hardware set-up; (b) Information flow

The trajectory pixel data input is converted by the camera into trajectory coordinates (x,y). The azimuth and elevation angles of the TDOF manipulator are computed using inverse kinematic and then the robot is driven by the motors so that the heading direction of the tip pin points to the trajectory coordinates by a laser pointer. The laser point (object) coordinates (x,y) and its distance is read by the camera. The trajectory pixel data output is compared with the trajectory pixel data input, Figure 6 plots the trajectory data input (kx, ky, kz).

In practice, the microcontroller receives decimal values corresponding to the reference angle values from the host computer. In the experimental set up the following unit conversion holds: 1 pixel = 0.00176 cm = 0.00172 rad = 0.0984 deg. The resolution of the input-output signal is 10 bits. From calibration through direct measurement, the relationship between angle and decimal value is given as follows:

$$D_{az} = -0.0002\theta_1^3 + -0.0001\theta_1^2 + 1.1492\theta_1 + 524.36 \quad (15)$$

$$D_{el} = -0.0004\theta_2^2 + 3.9254\theta_2 + 530.08 \quad (16)$$

where D_{az} is a decimal value to enable azimuth rotation pulse, and D_{el} is a decimal value to enable elevation rotation pulse. The default position (0,0) of the TDOF manipulator in decimal is 526 (azimuth) and 530 (elevation).

VI. Result and Analysis

A computer code has been made using C language to implement the algorithm. Figure 7 shows experiment results of aiming direction

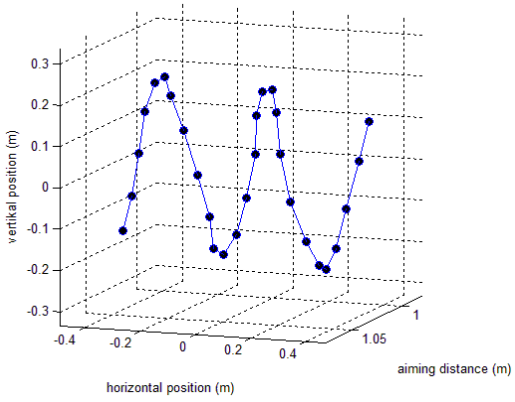

Figure 6. Isometric view of trajectory input

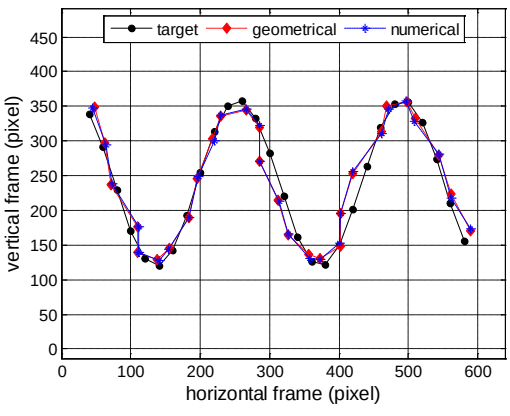

Figure 7. Experiment results

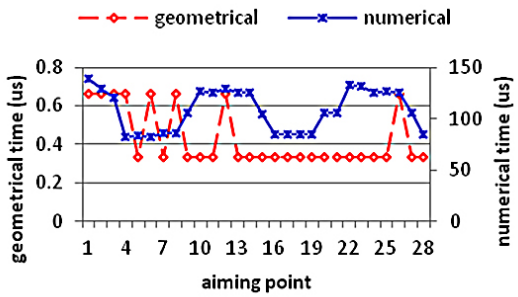

Figure 8. Processing time during experiment

with 28 pieces of target coordinates. The solid black line is the reference target coordinates generated by equation (18), the broken red line is output coordinates using geometrical approach, and the solid blue line is the output coordinate using numerical approach.

Performance indicators of the error signal, *i.e.* average value (μ) and standard deviation (σ), are listed in Table 2. Processing time consumed by the host computer during the experiment was also recorded, and shown in Figure 8. The maximum processing time required to calculate the inverse kinematic is 0.7 μs for geometrical approach and 139.0 μs for the numerical approach. Average processing times of geometrical and numerical approaches are 0.4 μs and 108.4 μs, respectively. It can be said that the processing time of the numerical approach is 250 times longer than the geometrical approach.

The experiment result has been further analized in the form of aiming error as shown in Figure 9. From Figure 9, it can be seen that the results of the aiming fall into the scope of the field tested, in other words, it has high accuracy and precision. By substituting performance indicator values in Table 2 into equation 17, relative accuracy percentage is obtained which is 98.55% for geometrical approach and 98.63% for the numerical approach.

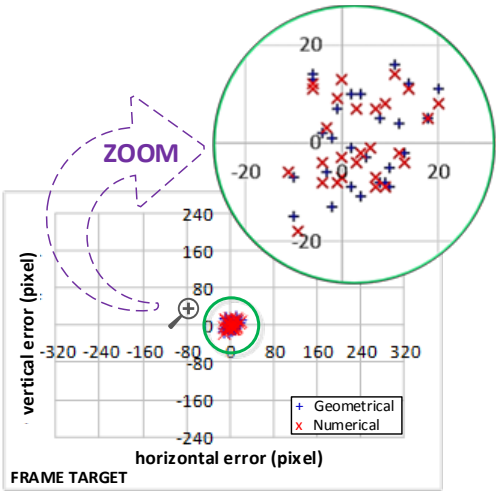

Figure 9. Aiming error

The experiment results were also analyzed statistically. Table 3 shows the details of statistical tests and values from CEP test data. It gives confidence level of 90% (α = 0.1). The statistical tests show generally good results. Special to the MPI test at the target, the population distribution at X axis produces critical t < t statistical which means it rejects the null hypothesis. However, since p-value > 0.1 (90%), this does not provide evidence to reject the null hypothesis that the MPI is not at the targets.

The CEP plots can be seen in Figure 10. It appears that the CEP (50% probable) for the numerical approach is smaller than the geometrical approach, *i.e.* 10.27 pixels and 9.79 pixels, respectively.

Table 2.
Performance indicators of error signal

Parameter	Geometrical		Numerical	
	X	Y	X	Y
mean, μ	3.50	-0.11	3.32	0.29
deviation standard, σ	8.28	9.17	8.09	8.54
count, n	28.00	28.00	28.00	28.00
degree of freedom, d_f	27.00	27.00	27.00	27.00
$k = \sigma_{min}/\sigma_{max}$	0.90		0.95	

Table 3.
CEP statistical test details

CEP Results at (α = 0,01)	Geometrical (pixel)		Numerical (pixel)	
	Az	El	Az	El
t-Test for statistical independence				
σ^2	68.63	84,10	65.41	72.88
$\hat{S}^2_{pooled}$	76.36		69.14	
d_f	54.00		54.00	
t statistical	1.54		1.37	
t critical	1.67		1.67	
Independent:	**YES**		**YES**	
Lilliefors Test for normality				
t statistical	0.10	0.13	0.1	0.14
t critical	0.15		0.15	
Bivariate normal:	**YES**		**YES**	
t-Test for MPI at target				
t statistical	2.24	0.06	2.17	0.18
t critical	0.15		0.15	
MPI at the target:	NO	**YES**	NO	**YES**
p-value	0.98	0.52	0.98	0.57
F-Test for circular distribution				
F statistical	0.60		0.78	
F critical	1.65		1.65	
Circular:	**YES**		**YES**	
CEP Results				
CEP (about MPI)	10,27		9,79	

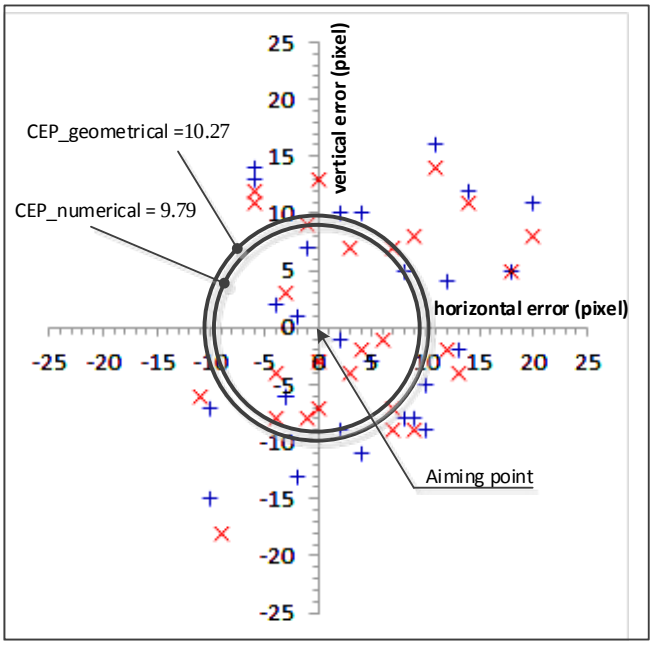

Figure 10. CEP result

VII. CONCLUSION

The research proves that numerical method provides relative accuracy percentage which is better than geometric method, which is equal to 98.63% and 98.55%, respectively. Therefore, it can be recommended to implement the numerical algorithm into TDOF robot manipulator instead of the geometrical one.

ACKNOWLEDGEMENT

This work was supported by the Research Center for Electrical Power and Mechatronics - LIPI, Indonesia.The authors would like to thank Aditya Sukma Nugraha M.T. who helped in the manufacture of the TDOF mechanism. Thanks also to Dr. Maria Margaretha Suliyanti who guided scientific paper writing.

REFERENCES

[1] M. Mirdanies, *et al.*, "Object Recognition System in Remote Controlled Weapon Station using SIFT and SURF Methods," *Mechatronics, Electrical Power, and Vehicular Technology*, vol. 4, no. 2, pp. 99-108, 2013.

[2] J. J. Craig, *Introduction to Robotics: Mechanics and Control*. Third penyunt., Canada: Pearson Prentice Hall, 2005.

[3] H. M. Saputra, *et al.*, "Analysis of Inverse Angle Method for Controlling Two Degree of Freedom Manipulator," *Mechatronics, Electrical Power, and Vehicular Technology*, vol. 3, no. 1, pp. 9-16, 2012.

[4] H. M. Saputra, "Simulation of 2-DOF Mechanism Control System for Satellite Communication Antennas, " Master Thesis, Aerospace and Mechanical Department, Institut Teknologi Bandung (ITB), Bandung, 2012.

[5] H. M. Saputra and E. Rijanto, "Analisis Kinematik dan Dinamik Mekanisme Penggerak 2-DOF untuk Antena Bergerak pada Komunikasi Satelit (Kinematic and dynamic analysis of a 2-DOF mechanism for mobile satellite communication (SATCOM) antennas)," *Teknologi Indonesia*, vol. 32, pp. 21-29, 2009.

[6] A. Aristidou and J. Lasenby, "Inverse Kinematics: A Review of Existing Techniques and Introduction of a New Fast Iterative Solver," University of Cambridge, Technical Report CUED/F-INFENG/TR-6322009, 2009.

[7] Y. Feng, *et al.*, "Inverse Kinematic Solution for Robot Manipulator Based on Electromagnetism-like and Modified DFP Algorithms," *Acta Automatica Sinica*, vol. 37, no. 1, pp. 74-82, 2011.

[8] K. Tchon, *et al.*, "Approximation of Jacobian Inverse Kinematics Algorithms," *Int. J. Appl. Math. Comput. Sci*, vol. 19, no. 4, pp. 519-531, 2009.

[9] M. Soch and R. Lorencz, "Solving Inverse Kinematics–A New Approach to the Extended Jacobian Technique," *Acta Polytechnica*, vol. 45, no. 2, pp. 21-26, 2005.

[10] R. Taufiq, "*Perancangan penelitian dan analisis data statistika*, " Penerbit ITB, Bandung, 2006.

[11] M. C. Anderson, "Generalize Weapon Effectiveness Modeling," Naval

Postgraduate School, Monterey, California, 2004.

[12] T. R. Jorris, *et al.*, "Design of Experiments and Analysis Examples from USAF Test Pilot School," *US Air Force T&E Days Conference* Nashville, Tennessee, pp. 337-363, 2010.

[13] C. McMillan and P. McMillan, "Characterizing rifle performance using circular error probable measured via a flatbed scanner," Version 1.01 Ed: Creative Commons Attribution-Noncommercial-No Derivative Works 3.0 United States License, 2008.

[14] Y. Wang, *et al.*, "Comprehensive Assessment Algorithm for Calculating CEP of Positioning Accuracy," *Measurement*, vol. 47, pp. 255-263, 2014.

[15] A. Didonato, "Computation of the Circular Error Probable (CEP) and Confidence Intervals in Bombing Test," Dahlgren Division Naval Surface Warfare Center NSWCDD/TR-07/13, Dahlgren, Virginia, 2007.